

# Studies of Vibrational Properties in Ga Stabilized $\delta$ -Pu by Extended X-ray Absorption Fine Structure

P. G. Allen,\* A. L. Henderson, and E. R. Sylwester  
*Seaborg Institute for Transactinium Science, Lawrence Livermore  
National Laboratory, P.O. Box 808, Livermore, California 94551*

P. E. A. Turchi, T. H. Shen, and G. F. Gallegos  
*Materials Science and Technology Division, Lawrence Livermore  
National Laboratory, P.O. Box 808, Livermore, California 94551*

C. H. Booth

*Chemical Sciences Division, Lawrence Berkeley National Laboratory, Berkeley, California 94720*

(Dated: Phys. Rev. B in press as of April 15, 2002)

Temperature dependent extended x-ray absorption fine structure (EXAFS) spectra were measured for a 3.3 at% Ga stabilized Pu alloy over the range  $T = 20 - 300$  K. EXAFS data were acquired at both the Ga  $K$ -edge and the Pu  $L_{III}$ -edge. Curve-fits were performed to the first shell interactions to obtain pair-distance distribution widths,  $\sigma$ , as a function of temperature. The temperature dependence of  $\sigma(T)$  was accurately modeled using a correlated-Debye model for the lattice vibrational properties, suggesting Debye-like behavior in this material. Using this formalism, we obtain pair-specific correlated-Debye temperatures,  $\Theta_{cD}$ , of  $110.7 \pm 1.7$  K and  $202.6 \pm 3.7$  K, for the Pu-Pu and Ga-Pu pairs, respectively. The result for the Pu- $\Theta_{cD}$  value compares well with previous vibrational studies on  $\delta$ -Pu. In addition, our results represent the first unambiguous determination of Ga-specific vibrational properties in PuGa alloys, i.e.,  $\Theta_{cD}$  for the Ga-Pu pair. Because the Debye temperature can be related to a measure of the lattice stiffness, these results indicate the Ga-Pu bonds are significantly stronger than the Pu-Pu bonds. This effect has important implications for lattice stabilization mechanisms in these alloys.

PACS numbers: 61.10.Ht, 61.66.Dk, 63.20Dj

## I. INTRODUCTION

Plutonium in its elemental form presents a complicated picture of phase stability.<sup>1</sup> Indeed, Pu may adopt one of six crystallographically different phases ( $\alpha$ ,  $\beta$ ,  $\gamma$ ,  $\delta$ ,  $\delta'$ , and  $\epsilon$ ) upon heating from room temperature to its melting point of 913 K. This complex phase behavior has been explained, in part, by the behavior of the Pu  $5f$  orbitals which fluctuate between itinerant and localized behavior. In this heuristic framework, elemental Pu represents the transition point along the actinide series from the delocalized electronic nature of the early actinides (Ac-Np) to localized, lanthanide-like  $f$ -orbital character observed for the heavier actinides.<sup>2</sup> Theoretical calculations currently support the hypothesis that the  $5f$  orbitals are delocalized for elements lighter than Pu in the actinide series and localized for those heavier than Pu.<sup>3</sup> This view of the relationship between electronic and crystallographic structure is reinforced by comparing the complex phase behavior and structures observed for pure U, Np, and Pu metals as opposed to the relatively simple structures observed for the elements Am and beyond.

The structural and electronic relationships that exist between the  $\alpha$  and  $\delta$  phases have received much attention due to some unusual observations. Pure face-centered cubic (fcc)  $\delta$ -Pu is stable from 593 to 736 K, and exhibits a 25% increase in volume relative to that of the ground state phase,<sup>1</sup> monoclinic  $\alpha$ -Pu. However, it is well known

that the fcc structure can be stabilized down to ambient temperature by the addition of small amounts ( $\sim 3-9$  at%) of alloying elements such as Al, Ga, In, Sc, and Ce.<sup>4</sup> However at lower impurity atom concentrations, the  $\delta$  phase converts directly to the  $\alpha$  form upon cooling, possibly through a martensitic phase transformation.<sup>5,6</sup>

Other than a tendency to form trivalent cations, relatively little is known about the mechanism of these so-called “ $\delta$ -stabilizers”.<sup>7,8</sup> Band structure studies have suggested that Al, Ga and Sc impurities diffuse the  $5f$  bands, thereby removing their involvement in bonding and leading to the stability of a more common,  $d$ -bonded transition metal-like phase.<sup>9</sup> Becker *et al.* have employed an ab initio LDA approach to study the lattice relaxation in a  $\text{Pu}_{31}\text{Ga}$  supercell cluster, and find evidence of a lattice contraction around the Ga site which relaxes the bonding constraints for the neighboring Pu atoms.<sup>10</sup> Other theoretical works<sup>11</sup> point to a substantial level of  $5f$  localization in the  $\delta$ -phase<sup>12</sup> and have speculated on a Kondo-like model for the involvement of the  $5f$  electrons.<sup>13</sup>

Analysis of the vibrational properties in these materials is also important for understanding  $\delta$ -phase stabilization. Unfortunately, measurement of the phonon dispersion using conventional inelastic neutron scattering techniques is troublesome given the difficulty in growing high-quality single crystals. An alternative approach is to evaluate the Debye temperature,  $\Theta_D$ , using various structural techniques. Ledbetter *et al.*<sup>14</sup> employed ultra-

sonic wave measurements of elastic constants for 3.3 at% Ga  $\delta$ -Pu and calculated a  $\Theta_D$  value of 115 K. The thermal behavior of 5.0 at% Al  $\delta$ -Pu was studied by temperature-dependent neutron powder diffraction<sup>15</sup> yielding a similarly low value of  $\Theta_D=132$  K. More recently, Lynn *et al.*<sup>16</sup> studied a 3.6 at% Ga  $\delta$ -Pu sample using neutron-resonance Doppler spectroscopy, a technique that can determine element specific values for  $\Theta_D$ . The experiments determined a Pu-specific value of  $\Theta_D=127$  K, and assigned a Ga specific value of  $\Theta_D=255$  K, although with relatively large errors ( $\pm 22$  K). As a test of the Debye model, one can check the assumption of equal force constants for the Pu and Ga sites by comparing the Ga- $\Theta_D$  to the  $\sqrt{m_{\text{Pu}}/m_{\text{Ga}}}$  weighted value of 236 K derived from the Pu- $\Theta_D$  value. Thus, this comparison does not exclude the possibility that the Ga atoms experience a stiffer force field compared with the Pu atoms.

In this article, we present temperature dependent EXAFS (extended x-ray absorption fine-structure) spectroscopic results for 3.3 at% Ga  $\delta$ -Pu as a means of discerning differences in the vibrational character of the Ga and Pu sites. Previously, EXAFS studies on Ga stabilized  $\delta$ -Pu have focused on isothermal measurements at either the Ga  $K$ - or the Pu  $L_{\text{III}}$ -edges, and have revealed some important effects.<sup>17-19</sup> In general, these studies indicate that the Ga atoms reside in their expected fcc lattice positions although there is an appreciable lattice contraction observed for the Ga-Pu bonds ( $\sim 3$ -4%). Surprisingly, the contraction in Ga-Pu bonds is significantly larger than the collapse calculated theoretically<sup>10</sup> or the contraction expected from Vegard's law based on a simple substitutional alloy. In addition, EXAFS data show increased disorder for the Pu-Pu near neighbor interactions. These results indicate that there are unexpected, site-specific lattice effects occurring in these materials.

The outline of the paper is as follows: details of sample preparation and EXAFS experimental setup and data analysis are discussed in Sec. II. The results of curve-fitting analysis and modeling the  $\sigma(T)$  temperature dependence using the correlated Debye model are presented in Sec. III. A discussion of the results and their relation to other  $\Theta_D$  studies is presented in Sec. IV, and the conclusions are given in Sec. V.

## II. EXPERIMENTAL DETAILS

### A. Sample Preparation

A  $\sim 6$   $\mu\text{m}$  thick <sup>239</sup>Pu foil (3.3 at % Ga) was prepared from 20 year old material by melting to remove accumulated helium, followed by subsequent annealing, cutting, and rolling. The foil was further homogenized at 450 °C for  $\sim 100$  hrs to ensure that single-phase,  $\delta$ -Pu was produced. Transmission x-ray diffraction was performed at LLNL and confirmed the presence of the fcc phase, with no significant amounts of other Pu phases present. In preparation for EXAFS analysis, the foil was electropol-

ished to remove any accumulated oxide material on the surface. The sample was then encapsulated under argon using a specially designed, triple containment x-ray compatible cell manufactured by Boyd Tech. The first level of containment consisted of coating the sample in a thin film of liquid polyimide solution that was allowed to air dry directly on the sample. The foil was then mounted onto an aluminum frame and sealed within two additional layers of x-ray transparent Kapton windows (0.010" thick). The windows were clamp-mounted onto the aluminum body with stainless steel window frames and using indium wire as a vacuum seal material. The triple-contained sample was subsequently mounted in an open cycle liquid helium flow-cryostat for variable temperature EXAFS measurements. Temperature measurement errors are within  $\sim 1$  K, and are stable within  $\sim 0.2$  K.

### B. EXAFS Data Acquisition and Analysis

Plutonium  $L_{\text{III}}$ - and gallium  $K$ -edge x-ray absorption spectra were collected at the Stanford Synchrotron Radiation Laboratory (SSRL) on wiggler beamline 11-2 under normal ring operating conditions using a nitrogen-cooled Si (220), half-tuned, double-crystal monochromator operating in unfocussed mode. The vertical slit height inside the x-ray hutch was 0.3 mm which reduces the effects of beam instabilities and monochromator glitches while providing ample photon flux. The Pu  $L_{\text{III}}$ -edge spectra were measured in transmission mode using Ar-filled ionization chambers. The Ga  $K$ -edge spectra were measured in fluorescence mode using a 30-element Ge array solid state detector developed by Canberra Industries. The detector was operated at  $\sim 75$  kHz per channel, and the signals were digitally processed using the DXP 4C/4T developed by X-ray Instrumentation Associates.

XAFS raw data treatment, including calibration, normalization, and subsequent processing of the EXAFS and XANES (x-ray absorption near-edge structure) spectral regions was performed by standard methods reviewed elsewhere<sup>20,21</sup> using the EXAFSPAK suite of programs developed by G. George of SSRL. Typically, three XAFS scans (transmission or fluorescence) were collected from each sample at each temperature and the results were averaged. The spectra were energy calibrated by simultaneously measuring the absorption spectrum for the reference samples PuO<sub>2</sub> or Ga<sub>2</sub>O<sub>3</sub>. The energies of the first inflection points for the reference sample absorption edges,  $E_r$ , were defined at 18053.1 eV (Pu  $L_{\text{III}}$ ) and 10368.2 eV (Ga  $K$ ). The EXAFS threshold energies,  $E_0$ , were defined as 18070 eV and 10385 eV for the Pu and Ga edges, respectively. Nonlinear least-squares curve-fitting was performed on the  $k^3$ -weighted EXAFS data using the EXAFSPAK programs.

The EXAFS data were fit using theoretical phase and amplitude functions calculated from the program FEFF8.1 of Rehr *et al.*<sup>22,23</sup> All of the Pu-Pu interactions

were modeled using single scattering (SS) paths derived from the model compound, unalloyed  $\delta$ -Pu,  $a_{\text{fcc}}=4.6371$  Å.<sup>24</sup> The Ga-Pu SS interactions were modeled by using the same model compound structure and replacing the central absorbing atom with Ga. An initial series of fits was done on the raw Pu  $L_{\text{III}}$  and Ga  $K$ -edge  $k^3$ -weighted data sets using the expected fcc near-neighbor interactions at 3.28, 4.64, 5.68, and 6.56 Å and fixing the coordination numbers at 12, 6, 24, 12, and 24, respectively. The results (especially at low T) confirmed the presence of the fcc structure and showed no evidence for other unusual structural effects. That is, we observed no phase changes (i.e.,  $\delta \rightarrow \alpha$ ) or previously postulated metastable impurity phases.<sup>25,26</sup> This first level of analysis was also used to establish values for  $S_0^2$  and  $\Delta E_0$  by fixing coordination numbers,  $N$ , and allowing  $S_0^2$ ,  $\Delta E_0$ ,  $\sigma^2$ , and  $R$  to vary. The final values used were taken from averaging over the range of temperatures studied: for Pu  $S_0^2 = 0.55$ ,  $\Delta E_0 = -12$  eV; and for Ga,  $S_0^2 = 0.85$ ,  $\Delta E_0 = -10$  eV.

As a result of the preliminary analyses, all of the subsequent fits described here focussed on isolating the behavior of the first shell Pu-Pu and Ga-Pu interactions in a highly constrained manner. Thus fits were done on Fourier-filtered data using the same fixed  $S_0^2$  and  $\Delta E_0$  values for all temperatures, along with a fixed coordination number of  $N=12$  for the first shell. The ability to fix  $\Delta E_0$ ,  $N$ , and  $S_0^2$  helps to avoid correlation problems between the fit parameters and to establish more consistently any changes in  $\sigma^2$  and  $R$  that may occur as functions of temperature.

### III. RESULTS

#### A. EXAFS Raw Data and Curve-Fitting

Figures 1A and 1B show the raw  $k^3$ -weighted Pu EXAFS  $L_{\text{III}}$  data and the corresponding Fourier transforms (FT) for the  $\delta$ -Pu sample as a function of temperature. The FT represents a pseudo-radial distribution function and the peaks are shifted to lower  $R$  values compared to real interaction values as a result of the phase shifts associated with the absorber-scatterer interactions ( $\sim 0.1$ - $0.2$  Å for Pu-Pu). As the sample is cooled from 293 K to 20 K, the EXAFS scattering amplitude increases systematically due to decreased thermal motion of the atoms in the lattice. As a result, the effective measurable  $k$ -range increases substantially at lower temperature. This effect is equally visible in the corresponding FTs. As the temperature is lowered, the intensity of the FT peaks increases dramatically, and the spectra reveal a pattern consistent with that expected for a fcc lattice. The first shell Pu-Pu peak seen at  $\sim 3.1$  Å corresponds to 12 Pu near neighbors in the fcc structure and increases in maximum peak height while also narrowing with decreasing temperature. The second, third, and fourth shell peaks at  $\sim 4.4$ , 5.4 and 6.3 Å which correspond to real inter-

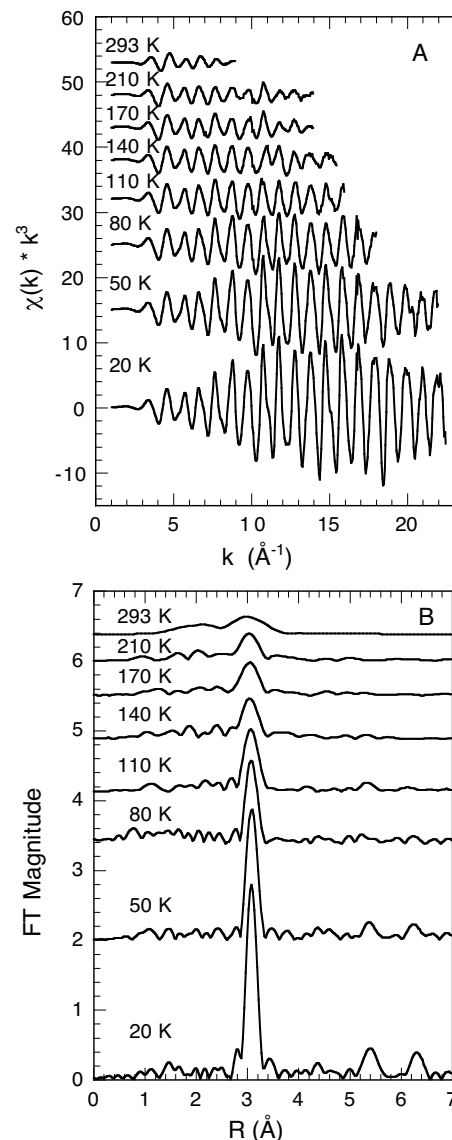


FIG. 1: Pu  $L_{\text{III}}$ -edge  $k^3$ -weighted EXAFS data (A) and the corresponding Fourier transforms (B) for the  $\delta$ -Pu sample as a function of temperature. Data were acquired in transmission mode and Fourier transformed over the ranges shown in the figure.

actions at 4.64, 5.68, and 6.56 Å are clearly affected by thermal effects and become distinguishable only below 80 K.

The Ga  $K$ -edge raw  $k^3$ -weighted EXAFS and corresponding FTs are shown in Figures 2A and 2B. This series of spectra qualitatively exhibit the same thermal behavior observed in the Pu  $L_{\text{III}}$ -edge EXAFS data, that is, increased scattering amplitude along with detection of more distant neighbors are apparent with decreasing temperature. The spectra are dominated by the peak at  $\sim 3.0$  Å, attributed to the first shell Ga-Pu interactions ( $N=12$ ). At lower temperatures, the FTs reveal second, third, and fourth shell Pu neighbor interactions

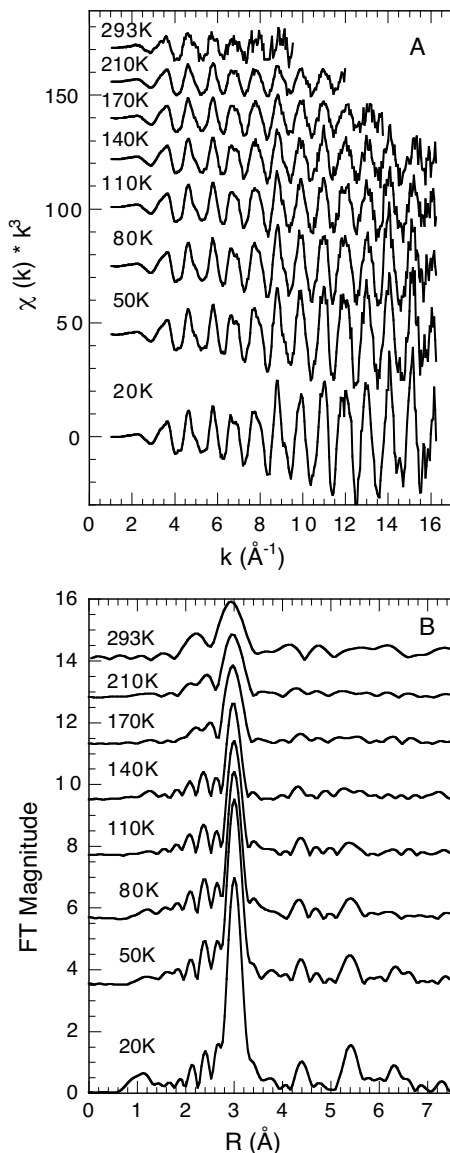


FIG. 2: Ga  $K$ -edge  $k^3$ -weighted EXAFS data (A) and the corresponding Fourier transforms (B) for the  $\delta$ -Pu sample as a function temperature. Data were acquired in fluorescence mode and Fourier transformed over the ranges shown in the figure.

at  $\sim 4.4, 5.4, 6.3$  Å, respectively. In contrast to the behavior observed in the Pu EXAFS, the detection of these longer range interactions is retained up to higher temperatures (ca. 110 K). At this level of analysis, this observation suggests that the Ga-Pu interactions experience less thermal broadening than the corresponding Pu-Pu interactions, which is especially surprising given the decreased reduced mass of the Ga-Pu pair relative to the Pu-Pu pair.

Following initial inspection of the data (see Section II) we chose to focus our analyses on the isolated first shell contributions, in part, due to the high signal-to-noise

TABLE I: Pu  $L_{III}$  and Ga  $K$ -edge EXAFS single shell curve fitting results. The first shell interactions were isolated by Fourier transforming over the data  $k$ -ranges displayed in Figures 1A and 2A, and back-transforming over the range  $R=2-4$  Å. Several parameters were held fixed as follows: for Pu and Ga,  $N=12$ ; for Pu,  $S_0^2 = 0.55$  and  $\Delta E_0 = -12$  eV; and for Ga,  $S_0^2 = 0.85$  and  $\Delta E_0 = -10$  eV.

Sample	Pu-Pu shell <sup>a</sup>		Ga-Pu shell		
	Temp (K)	$R$ (Å)	$\sigma^2$ (Å <sup>2</sup> )	$R$ (Å)	$\sigma^2$ (Å <sup>2</sup> )
20		3.290	0.00280	3.160	0.00275
50		3.292	0.00381	3.160	0.00332
80		3.293	0.00511	3.160	0.00395
110		3.301	0.00680	3.160	0.00512
140		3.301	0.00905	3.160	0.00609
170		3.306	0.01039	3.163	0.00764
210		3.316	0.01275	3.165	0.00953
293		3.297	0.01821	3.171	0.01264

<sup>a</sup>Errors in  $R$  and  $\sigma^2$  are estimated to be  $\pm 0.005$  Å and  $\pm 10\%$  based on EXAFS fits to known model compounds, cf. Ref. 21.

obtained relative to the more distant shell interactions. Thus by curve-fitting the Fourier-filtered first shell components from the Pu  $L_{III}$  and Ga  $K$  EXAFS, the local vibrational temperature dependence may be investigated. The first shell interactions were isolated by Fourier transforming over the data  $k$ -ranges shown in Figures 1A and 2A, and back-transforming over the range  $R=2-4$  Å.

The curve-fitting results summarized in Table I serve to identify the different temperature dependent and static structural effects for the Pu and Ga sites in this material. Figure 3 shows the resulting curve fits to the Fourier filtered Pu and Ga EXAFS data measured at 20 K in  $k$ -space and  $R$ -space. The strong coincidence between the data and the fits serves to illustrate the highly refined nature of the FEFF8.1 calculations as well as the appropriateness of the fitting procedure employed. Because these fits were highly constrained, any changes in the data are assigned to changes in  $R$  and  $\sigma^2$ . The first effect revealed by these data is the overall contraction of Pu atoms around the Ga sites relative to the environment around the Pu sites. This “collapse” of about 4% is comparable to that observed by earlier EXAFS studies on  $\delta$ -Pu.<sup>17-19</sup> The first shell bond lengths for each element appear to remain constant over the measured temperature range, at least within the quoted experimental error and under the constraints outlined above.

## B. Vibrational Analysis

The most dramatic effect depicted in this data set is the difference in the temperature dependence between the Pu-Pu and Ga-Pu Debye-Waller factors,  $\sigma^2$ . The values for  $\sigma^2$  increase with temperature consistent with greater thermal disorder, as expected. However, according to Table I, the Pu-Pu first shell shows much greater disorder at higher temperature than the corresponding

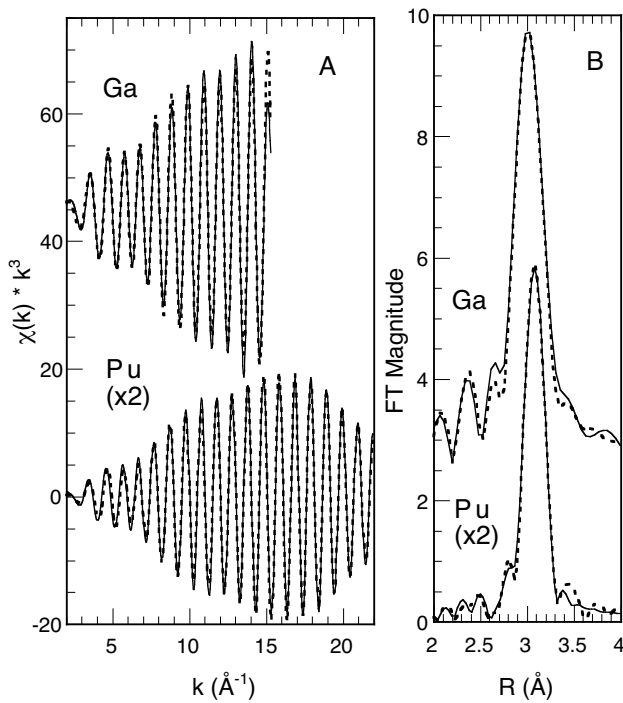


FIG. 3: Representative single shell curve fits (dotted lines) to the Pu  $L_{III}$  and Ga  $K$ -edge data (solid lines) measured at 20K in (A)  $k$ -space and (B)  $R$ -space. Data were Fourier-filtered from the raw spectra over the  $k$  and  $R$  ranges shown in the plots using Gaussian window functions with half-widths of  $0.5 \text{ \AA}^{-1}$  and  $0.05 \text{ \AA}$ , respectively. Pu data shown are multiplied by a factor of 2 for the purpose of comparison to the Ga data.

Ga-Pu shell. Moreover, this occurs in spite of the fact that the Ga-Pu pair has a lower reduced mass. To study this effect more carefully, the temperature dependence of the Debye-Waller factors was modeled by employing the correlated-Debye Model to determine the Debye Temperature.<sup>27</sup>

$$\sigma_{meas}^2(T) = \sigma_{static}^2 + F(T, \theta_{cD}). \quad (1)$$

The temperature-dependent part of the Debye-Waller factor  $F(T, \theta_{cD})$  is given within the correlated-Debye model by

$$F(T, \theta_{cD}) = \frac{\hbar}{2\mu} \int \rho_j(\omega) \coth\left(\frac{\hbar\omega}{2k_B T}\right) \frac{d\omega}{\omega}$$

where  $\mu$  is the reduced mass,  $\theta_{cD}$  is the correlated Debye temperature, and the phonon density of states at position  $R_j$  is<sup>28</sup>

$$\rho_j = \frac{3\omega^2}{\omega_D^3} \left[ 1 - \frac{\sin(\omega R_j/c)}{\omega R_j/c} \right] \quad (2)$$

in which  $\omega_D$  is the usual Debye frequency and  $c = \omega_D/k_B$  where  $k_B$  is Boltzmann's constant. The expression in brackets of Eq. 2 takes into account the correlated motion of the atom pairs.

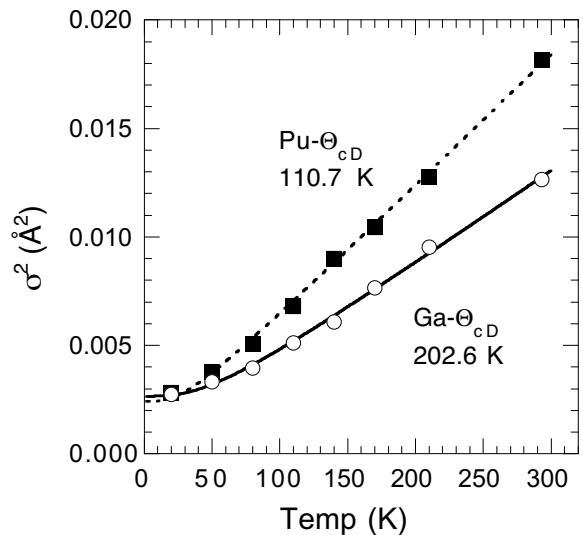


FIG. 4: Temperature dependence of EXAFS Debye-Waller factors for first shell Pu-Pu (upper data) and Ga-Pu (lower data) interactions plotted along with fits generated using the correlated Debye model.

Using this formalism, we obtain the fits shown in Figure 4, and determine pair-specific correlated-Debye Temperatures,  $\Theta_{cD}$ , of  $110.7 \pm 1.7 \text{ K}$  and  $202.6 \pm 3.7 \text{ K}$ , for the Pu and Ga sites, respectively. Estimates of the  $\sigma_{static}^2$  parameter are all consistent with no static disorder, and fall in the range of  $0.0003 \pm 0.0003 \text{ \AA}^2$ . The data appear to fit this model quite accurately, indicating that the local pair vibrations can be described using the correlated-Debye model. However, the higher  $\Theta_{cD}$  of the Ga-Pu pair with respect to the Pu-Pu pair may indicate the presence of a local lattice anomaly from a vibrational standpoint, which could be related to the observed lattice contraction measured around the Ga sites.

#### IV. DISCUSSION

It is instructive to compare the EXAFS  $\Theta_{cD}$  results described here with those obtained from previous studies. Table II summarizes the  $\Theta_D$  values for  $\delta$ -Pu determined from our study along with those from earlier works. We also make special note of the differences in the methods used to determine these values, which is important for a proper interpretation. The elastic values of  $\Theta_D$  are obtained by ultrasound measurements of “bulk” lattice wave properties extrapolated down to  $T=0 \text{ K}$ .<sup>14,29,30</sup> The “Bulk Modulus” value uses a theoretical relationship<sup>31</sup> where  $\Theta_D = 41.63 \sqrt{r_0 B/M}$  to derive  $\Theta_D$  from an experimental value for  $B=450 \text{ kbar}$ . The  $\Theta_D$  value from neutron diffraction also represents a bulk measurement of lattice thermal behavior.<sup>15</sup> However, since it is derived from thermal displacement factors specifically attributed to the Pu atoms, it is referenced as  $\Theta_{DW}$ . The  $\Theta_D$  values obtained from EXAFS and neutron resonant

TABLE II: Comparison of Pu and Ga Specific Debye Temperatures Obtained for  $\delta$ -Pu by Various Techniques

$\delta$ -Pu alloy	Pu- $\Theta_D$	Ga- $\Theta_D$	Method
3.3 at% Ga	110.7		EXAFS
		202.6	EXAFS
	127		Neut. Abs. <sup>a</sup>
		255	Neut. Abs.
6.6 at% Ga	105		Bulk Mod. <sup>b</sup>
	115		Elastic <sup>c</sup>
5.0 at% Ga	127		Elastic <sup>d</sup>
	132		Elastic <sup>e</sup>
	132		Neut. Diff. <sup>f</sup>

<sup>a</sup>Neutron Resonance Doppler spectroscopy, Ref. 16.

<sup>b</sup>Using the relation from Ref. 31 and the experimental bulk modulus noted in the text.

<sup>c</sup>Ultrasonic measurement of 3 principal elastic constants,  $C_{ij}$ , Ref. 14.

<sup>d</sup>Derived from Young's modulus,  $E$ , and torsional modulus,  $G$ , Ref. 29.

<sup>e</sup>Also derived from  $E$  and  $G$ , Ref. 30.

<sup>f</sup>Neutron diffraction, Ref. 15.

absorption<sup>16</sup> are distinct from those derived from the other methods in that they are element specific, yet there are important differences to be noted. EXAFS inherently measures only phonon modes that involve specific atom pairs (i.e., we must consider the reduced mass for the pair). In contrast, neutron resonance absorption measures the average of all modes associated with a single atomic species (i.e., only the mass of the absorbing atom must be considered).

In general the Pu specific values of  $\Theta_D$  obtained from all the techniques are similar in that they are all quite low, ranging from 104 to 132 K. It is not our intent to discuss these differences since they come from such a wide variety of techniques and variability in samples. The Ga-specific Debye temperatures do however require more careful discussion, in relation to the Pu-specific values. As mentioned in Sec. I, neutron resonant absorption found a Ga specific  $\Theta_D$  value of 255 K  $\pm$  22 K which, compared to the  $\sqrt{m_{Pu}/m_{Ga}}$  weighted value of 236 K, does not exclude a slightly stiffer force field than the one around the Pu sites. Analogously, EXAFS yields a Ga specific  $\Theta_{cD}$  of 202.6  $\pm$  3.7 K which may be compared to the expected value of 164 K (i.e., the  $\sqrt{\mu_{Pu}/\mu_{Ga}}$  weighted value). The observation of a significantly higher  $\Theta_{cD}$  for the Ga-Pu pair relative to that expected for a simple substitutional lattice model, coupled with the anomalously large lattice contraction around the Ga sites clearly suggest that the Ga sites reside in a significantly stronger force field. The shorter Ga-Pu bonds, in fact, inherently imply a strengthening of the Ga-Pu bonds relative to the Pu-Pu bonds.

Regarding factors that contribute to  $\delta$ -phase stabilization, these results are consistent with the Ga atoms having a significant influence on the local electronic structure. One obvious possibility is that charge transfer exists between the Ga  $pd$  states and the corresponding Pu

$df$  states. This orbital overlap will directly dictate the extent of lattice vibrational distortions and local geometry within the crystal structure, that is, with a preference towards a fcc lattice in the presence of Ga. Therefore, the results of this EXAFS study give the first unambiguous evidence for the impact of the vibrational properties on the local lattice effects.

From the results of this study, we may also estimate values for "pair-specific bulk moduli." Indeed, according to the empirical relation between bulk modulus and Debye temperature established by Moruzzi *et al.*<sup>31</sup>, we deduce from our calculated Debye temperatures for Pu and Ga values of 498 and 1666 kbar, respectively, for the bulk modulus. Since the Pu-Ga alloy we have been studying has a composition in the dilute limit, this implies that Pu is mostly surrounded by Pu atoms whereas each Ga site can be viewed as embedded in a Pu matrix. In addition, the bulk modulus of pure Ga metal as determined by theory,<sup>32</sup> 606 kbar, or experiment,<sup>33</sup> 613 kbar, is quite low in accordance with the low melting point of 308 K. Hence the dramatic difference between the two estimated bulk moduli provides an equivalent description for the increase in strength gained in going from Pu-Pu (or Ga-Ga bonds) to Ga-Pu bonds. This unusually large increase in stability of a Pu (Ga) matrix by addition of Ga (Pu) is reflected in the existence of very stable Pu-Ga compounds (i.e., large heats of formation), some of them exhibiting congruent melting. It would be interesting to extend this work to other alloy compositions to quantify more appropriately these findings and have a better understanding of the unusual synergistic effects due to alloying in Pu-Ga and related systems.

## V. CONCLUSION

New pair specific Debye temperatures for the Ga-Pu and Pu-Pu pairs in  $\delta$ -Pu were determined using a correlated-Debye model fit to temperature dependent EXAFS Debye-Waller parameters. Using this formalism, we obtain pair specific correlated-Debye temperatures,  $\Theta_{cD}$ , of 110.7  $\pm$  1.7 K and 202.6  $\pm$  3.7 K, for the Pu-Pu and Ga-Pu pairs, respectively. The results for the  $\Theta_{cD}$  Pu-Pu pair compare well with previous vibrational studies on  $\delta$ -Pu. In addition, our results represent the first unambiguous determination of Ga-specific vibrational properties, i.e, Ga-Pu  $\Theta_{cD}$ , in PuGa alloys. Because the Debye temperature can be related to a measure of the lattice stiffness, these results indicate that the Ga-Pu bonds experience a stronger force field than the corresponding Pu-Pu bonds. This effect has important implications for lattice stabilization mechanisms in these alloys. If the vibrational properties in  $\delta$ -Pu are dependent on the type of impurity, further studies of Debye temperatures with other "stabilizers" will be important for discerning key aspects of the stabilization mechanism.

### Acknowledgments

This work was performed under the auspices of the U.S. Department of Energy (DOE) by the University of California Lawrence Livermore National Laboratory under contract No. W-7405-Eng-48. This work was partially supported (C. H. B.) by the Office of Basic Energy

Sciences, Chemical Sciences Division of the U. S. DOE, Contract No. DE-AC03-76SF00098. The authors also wish to thank John Rehr and Alex Ankudinov for helpful discussions. This work was done (partially) at SSRL, which is operated by the Department of Energy, Division of Chemical Sciences.

- 
- \* Electronic address: [allen42@llnl.gov](mailto:allen42@llnl.gov)
- <sup>1</sup> W. N. Miner and F. W. Schonfeld, in *Plutonium Handbook*, edited by O. J. Wick (The American Nuclear Society, La Grange Park, IL, 1990), p. 33.
  - <sup>2</sup> J. L. Smith and E. A. Kmetko, *J. Less-Common Met.* **90**, 83 (1983).
  - <sup>3</sup> J. M. Willis and O. Eriksson, *Phys. Rev. B* **45**, 13879 (1992).
  - <sup>4</sup> P. Chiotti, V. V. Akhachinskij, I. Ansara, and M. H. Rand, *The Chemical Thermodynamics of Actinide Elements and Compounds* (The American Nuclear Society, International Atomic Energy Agency, Vienna, 1981), vol. 5, p. 231.
  - <sup>5</sup> P. H. Adler, G. B. Olson, M. F. Stevens, and G. F. Gallagos, *Acta Metall. Mater.* **40**, 1073 (1992).
  - <sup>6</sup> T. G. Zocco, M. F. Stevens, P. H. Adler, R. I. Sheldon, and G. B. Olson, *Acta Metall. Mater.* **38**, 2275 (1990).
  - <sup>7</sup> J. R. K. Gschneidener, R. O. Elliott, and V. O. Struebing, in *Plutonium 1960* (Cleaver-Hume, London, 1961), p. 99.
  - <sup>8</sup> P. H. Adler, *Metall. Trans. A* **22**, 2237 (1991).
  - <sup>9</sup> P. Weinberger, A. M. Boring, and J. Smith, *Phys. Rev. B* **31**, 1964 (1985).
  - <sup>10</sup> J. D. Becker, J. M. Wills, L. Cox, and B. R. Cooper, *Phys. Rev. B* **58**, 5143 (1998).
  - <sup>11</sup> P. E. A. Turchi, A. Gonis, N. Kioussis, D. L. Price, and B. R. Cooper, in *Proceedings of the International Workshop on Electron Correlations and Materials Properties*, edited by A. Gonis, N. Kioussis, and M. Ciftan (Kluwer Academic and Plenum Publishers, New York and London, 1999), pp. 531–537.
  - <sup>12</sup> M. Pénicaud, *J. Phys.: Condens. Matter* **9**, 6341 (1997).
  - <sup>13</sup> S. Méot-Reymond and J. M. Fournier, *J. Alloys and Comp.* **232**, 119 (1996).
  - <sup>14</sup> H. M. Ledbetter and R. M. Moment, *Acta Metall.* **24**, 891 (1976).
  - <sup>15</sup> A. Lawson, J. Goldstone, B. Cort, R. Sheldon, and E. Folyton, *J. Alloys and Comp.* **213**, 426 (1994).
  - <sup>16</sup> J. Lynn, G. Kwei, W. J. Trela, V. W. Yuan, B. Cort, R. J. Martinez, and F. Vigil, *Phys. Rev. B* **58**, 11408 (1998).
  - <sup>17</sup> L. Cox, R. Martinez, J. H. Nickel, S. Conradson, and P. Allen, *Phys. Rev. B* **51**, 751 (1995).
  - <sup>18</sup> P. Faure, B. Deslandes, D. Bazin, C. Tailland, R. Doukhan, J. M. Fournier, and A. Falanga, *J. Alloys and Comp.* **244**, 131 (1996).
  - <sup>19</sup> N. Richard, P. Faure, P. Rofidal, J. L. Truffier, and D. Bazin, *J. Alloys and Comp.* **271-273**, 879 (1998).
  - <sup>20</sup> T. M. Hayes and J. B. Boyce, in *Solid State Physics*, edited by H. Ehrenreich, F. Seitz, and D. Turnbull (Academic, New York, 1982), vol. 37, p. 173.
  - <sup>21</sup> G. G. Li, F. Bridges, and C. H. Booth, *Phys. Rev. B* **52**, 6332 (1995).
  - <sup>22</sup> J. J. Rehr, J. Mustre de Leon, S. I. Zabinsky, and R. C. Albers, *Phys. Rev. B* **44**, 4146 (1991).
  - <sup>23</sup> J. J. Rehr, J. Mustre de Leon, S. I. Zabinsky, and R. C. Albers, *J. Am. Chem. Soc.* **113**, 5135 (1991).
  - <sup>24</sup> F. H. Ellinger, *J. Metals* **8**, 1256 (1956).
  - <sup>25</sup> S. D. Conradson, *Appl. Spectrosc.* **52**, 252A (1998).
  - <sup>26</sup> S. D. Conradson, in *Los Alamos Science, No 26, Vol. II* (Los Alamos National Laboratory, Report No. LA-UR-00-4100, 2000), pp. 356–363.
  - <sup>27</sup> E. D. Crozier, J. J. Rehr, and R. Ingalls, in *X-Ray Absorption: Principles, Applications, Techniques of EXAFS, SEXAFS, XANES*, edited by D. Konigsberger and R. Prins (Wiley, New York, 1988), p. 373.
  - <sup>28</sup> G. B. Beni and P. M. Platzman, *Phys. Rev. B* **14**, 1514 (1976).
  - <sup>29</sup> J. C. Taylor, P. F. T. Linford, and D. J. Dean, *J. Inst. Metals* **96**, 178 (1968).
  - <sup>30</sup> M. Rosen, G. Frez, and S. Shtrikman, *J. Phys. Chem. Solids* **30**, 1063 (1969).
  - <sup>31</sup> V. L. Moruzzi, J. F. Janak, and K. Schwarz, *Phys. Rev. B* **37**, 790 (1988).
  - <sup>32</sup> P. E. A. Turchi, A. Gonis, and N. Kioussis, calculated for hypothetical fcc-based Ga using the FP-LMTO (Full-Potential Linear Muffin-Tin Orbital) method, unpublished work.
  - <sup>33</sup> R. W. G. Wyckoff, *Crystal Structures, 2nd ed.* (Wiley, New York, 1962), vol. 1, p. 22.